SEARCH FOR NEUTRINOS IN SUPER-KAMIOKANDE ASSOCIATED WITH GRAVITATIONAL-WAVE EVENTS GW150914 AND GW151226

K. Abe[1,32], K. Haga[1], Y. Hayato[1,32], M. Ikeda[1], K. Iyogi[1], J. Kameda[1,32], Y. Kishimoto[1,32], M. Miura[1,32], S. Moriyama[1,32], M. Nakahata[1,32], T. Nakajima[1], Y. Nakano[1], S. Nakayama[1,32], A. Orii[1], H. Sekiya[1,32], M. Shiozawa[1,32], A. Takeda[1,32], H. Tanaka[1], S. Tasaka[1], T. Tomura[1,32], R. Akutsu[2], T. Kajita[2,32], K. Kaneyuki[2,32,37], Y. Nishimura[2], E. Richard[2], K. Okumura[2,32], L. Labarga[3], P. Fernandez[3], F. d. M. Blaszczyk[4], J. Gustafson[4], C. Kachulis[4], E. Kearns[4,32], J. L. Raaf[4], J. L. Stone[4,32], L. R. Sulak[4], S. Berkman[5], C. M. Nantais[5], S. Tobayama[5], M. Goldhaber[6,37], W. R. Kropp[7], S. Mine[7], P. Weatherly[7], M. B. Smy[7,32], H. W. Sobel[7,32], V. Takhistov[7], K. S. Ganezer[8], B. L. Hartfiel[8], J. Hill[8], N. Hong[9], J. Y. Kim[9], I. T. Lim[9], R. G. Park[9], A. Himmel[10], Z. Li[10], E. O'Sullivan[10], K. Scholberg[10,32], C. W. Walter[10,32], T. Ishizuka[11], T. Nakamura[12], J. S. Jang[13], K. Choi[14], J. G. Learned[14], S. Matsuno[14], S. N. Smith[14], M. Friend[15], T. Hasegawa[15], T. Ishida[15], T. Ishii[15], T. Kobayashi[15], T. Nakadaira[15], K. Nakamura[15,32], Y. Oyama[15], K. Sakashita[15], T. Sekiguchi[15], T. Tsukamoto[15], A. T. Suzuki[16], Y. Takeuchi[16,32], T. Yano[16], S. V. Cao[17], T. Hiraki[17], S. Hirota[17], K. Huang[17], M. Jiang[17], A. Minamino[17], T. Nakaya[17,32], N. D. Patel[17], R. A. Wendell[17,32], K. Suzuki[17], Y. Fukuda[18], Y. Itow[19,20], T. Suzuki[19], P. Mijakowski[21], K. Frankiewicz[21], J. Hignight[22], J. Imber[22], C. K. Jung[22], X. Li[22], J. L. Palomino[22], G. Santucci[22], M. J. Wilking[22], C. Yanagisawa[22,38], D. Fukuda[23], H. Ishino[23], T. Kayano[23], A. Kibayashi[23], Y. Koshio[23,32], T. Mori[23], M. Sakuda[23], C. Xu[23], Y. Kuno[24], R. Tacik[25,34], S. B. Kim[26], H. Okazawa[27], Y. Choi[28], K. Nishijima[29], M. Koshiba[30], Y. Totsuka[30,37], Y. Suda[31], M. Yokoyama[31,32], C. Bronner[32], R. G. Calland[32], M. Hartz[32], K. Martens[32], Ll. Marti[32], Y. Suzuki[32], M. R. Vagins[7,32], J. F. Martin[33], H. A. Tanaka[33], A. Konaka[34], S. Chen[35], L. Wan[35], Y. Zhang[35], AND R. J. Wilkes[36]

(The Super-Kamiokande Collaboration)

[1] Kamioka Observatory, Institute for Cosmic Ray Research, University of Tokyo, Kamioka, Gifu 506-1205, Japan
[2] Research Center for Cosmic Neutrinos, Institute for Cosmic Ray Research, University of Tokyo, Kashiwa, Chiba 277-8582, Japan
[3] Department of Theoretical Physics, University Autonoma Madrid, E-28049 Madrid, Spain
[4] Department of Physics, Boston University, Boston, MA 02215, USA
[5] Department of Physics and Astronomy, University of British Columbia, Vancouver, BC V6T1Z4, Canada
[6] Physics Department, Brookhaven National Laboratory, Upton, NY 11973, USA
[7] Department of Physics and Astronomy, University of California, Irvine, Irvine, CA 92697-4575, USA
[8] Department of Physics, California State University, Dominguez Hills, Carson, CA 90747, USA
[9] Department of Physics, Chonnam National University, Kwangju 500-757, Korea
[10] Department of Physics, Duke University, Durham, NC 27708, USA
[11] Junior College, Fukuoka Institute of Technology, Fukuoka, Fukuoka 811-0295, Japan
[12] Department of Physics, Gifu University, Gifu, Gifu 501-1193, Japan
[13] GIST College, Gwangju Institute of Science and Technology, Gwangju 500-712, Korea
[14] Department of Physics and Astronomy, University of Hawaii, Honolulu, HI 96822, USA
[15] High Energy Accelerator Research Organization (KEK), Tsukuba, Ibaraki 305-0801, Japan
[16] Department of Physics, Kobe University, Kobe, Hyogo 657-8501, Japan
[17] Department of Physics, Kyoto University, Kyoto, Kyoto 606-8502, Japan
[18] Department of Physics, Miyagi University of Education, Sendai, Miyagi 980-0845, Japan
[19] Institute for Space-Earth Environmental Research, Nagoya University, Nagoya, Aichi 464-8602, Japan
[20] Kobayashi-Maskawa Institute for the Origin of Particles and the Universe, Nagoya University, Nagoya, Aichi 464-8602, Japan
[21] National Centre For Nuclear Research, 00-681 Warsaw, Poland
[22] Department of Physics and Astronomy, State University of New York at Stony Brook, Stony Brook, NY 11794-3800, USA
[23] Department of Physics, Okayama University, Okayama, Okayama 700-8530, Japan
[24] Department of Physics, Osaka University, Toyonaka, Osaka 560-0043, Japan
[25] Department of Physics, University of Regina, 3737 Wascana Parkway, Regina, SK S4S OA2, Canada
[26] Department of Physics, Seoul National University, Seoul 151-742, Korea
[27] Department of Informatics in Social Welfare, Shizuoka University of Welfare, Yaizu, Shizuoka 425-8611, Japan
[28] Department of Physics, Sungkyunkwan University, Suwon 440-746, Korea
[29] Department of Physics, Tokai University, Hiratsuka, Kanagawa 259-1292, Japan
[30] The University of Tokyo, Bunkyo, Tokyo 113-0033, Japan
[31] Department of Physics, University of Tokyo, Bunkyo, Tokyo 113-0033, Japan
[32] Kavli Institute for the Physics and Mathematics of the Universe (WPI), The University of Tokyo Institutes for Advanced Study, University of Tokyo, Kashiwa, Chiba 277-8583, Japan
[33] Department of Physics, University of Toronto, 60 St. George Street, Toronto, ON M5S 1A7, Canada
[34] TRIUMF, 4004 Wesbrook Mall, Vancouver, BC V6T2A3, Canada
[35] Department of Engineering Physics, Tsinghua University, Beijing, 100084, China
[36] Department of Physics, University of Washington, Seattle, WA 98195-1560, USA

ABSTRACT

We report the results from a search in Super-Kamiokande for neutrino signals coincident with the first detected gravitational-wave events, GW150914 and GW151226, as well as LVT151012, using a neutrino energy range

---

[37] Deceased.
[38] Also at BMCC/CUNY, Science Department, New York, NY, USA.

from 3.5 MeV to 100 PeV. We searched for coincident neutrino events within a time window of ± 500 s around the gravitational-wave detection time. Four neutrino candidates are found for GW150914, and no candidates are found for GW151226. The remaining neutrino candidates are consistent with the expected background events. We calculated the 90% confidence level upper limits on the combined neutrino fluence for both gravitational-wave events, which depends on event energy and topologies. Considering the upward-going muon data set (1.6 GeV–100 PeV), the neutrino fluence limit for each gravitational-wave event is 14–37 (19–50) cm^{-2} for muon neutrinos (muon antineutrinos), depending on the zenith angle of the event. In the other data sets, the combined fluence limits for both gravitational-wave events range from 2.4×10^4 to 7.0×10^9 cm^{-2}.

Key words: astroparticle physics – gravitational waves – neutrinos

1. INTRODUCTION

On 2015 September 14 at 09:50:45 UT, LIGO identified the first evident signal of a gravitational wave as a coincidence of two chirp signals observed by two distant independent interferometers (Abbott et al. 2016c). It has been suggested that the gravitational-wave event, namely, GW150914, was due to a merger of two black holes having masses of approximately 30 to 60 solar mass. After the announcement of the discovery by the LIGO team on 2016 February 11, many efforts to search for coincidences in the observational data in complementary experiments have been made (Abbott et al. 2016b); no astronomical counterpart has been identified, except a weak coincident excess reported by *Fermi* GBM ~0.4 s after GW159014 (Connaughton et al. 2016), although this result is controversial (Greiner et al. 2016). Because of the tremendous energies involved and the unknown nature of the region of the black hole merger, it is possible to imagine coincident production of neutrinos. For example, the possibility of high-energy neutrino emission from relativistic jets when an accretion disk is formed around the source has been discussed (Eichler et al. 1989; Woosley 1993). IceCube and ANTARES have searched for high-energy neutrinos above ~100 GeV in a time window of ± 500 s around the real-time alert for GW150914 issued by LIGO, but reported no positive evidence for coincident neutrino events (Adrián-Martínez et al. 2016).

Following this event the second gravitational-wave signal, GW151226, was reported (Abbott et al. 2016a). It was observed on 2015 December 26 at 03:38:53 UT and was predicted to be due to a merger of two black holes having masses of 14.2 and 7.5 solar mass. KamLAND reported no positive coincident neutrino events for both of these two gravitational-wave events (Gando et al. 2016).

We report the results of a search for neutrinos in coincidence with GW150914 and GW151226 in Super-Kamiokande (SK). It is a water Cherenkov detector located at 2700-meters-water-equivalent underground in Kamioka, Japan. A detailed description of the detector can be found elsewhere (Fukuda et al. 2003). In this detector, the Cherenkov ring pattern reconstruction identifies final state electron and muon direction and energy from which we infer the neutrino direction, flavor, and energy. Our search includes the neutrino energy region of 1–100 GeV, which is not covered by the previous searches with neutrino telescopes. Moreover, SK has unique sensitivity to MeV neutrinos either from a core-collapse supernova in the Local Group or from some other similarly efficient mechanism. The neutrino events with reconstructed energies above 100 MeV are categorized as the "high-energy data sample" in SK and are typically used to study atmospheric neutrinos and search for proton decay. Neutrino events with reconstructed energies down to 3.5 MeV are categorized as the "low-energy data sample" and are typically used to study solar neutrinos and

to search for core-collapse supernova neutrinos. The background events in the search for astrophysical neutrinos for the high-energy data sample are almost entirely atmospheric neutrinos, while radioactive impurities, spallation products from cosmic-ray muons, atmospheric and solar neutrinos are the main backgrounds in the low-energy data sample.

2. SEARCH METHOD AND RESULTS

2.1. High-energy Data Sample

The high-energy data samples consist of three distinct topologies: fully contained (FC), partially contained (PC), and upward-going muon (UPMU). FC neutrino events have reconstructed interaction vertices inside the fiducial volume with little light detected in the outer detector. PC neutrino events also have interaction vertices within the fiducial volume of the inner detector, but there is significant light in the outer detector volume. UPMU neutrino events are the highest-energy events in the SK detector and are due to muon neutrino interactions in the surrounding rock that produce penetrating muons. These muons either stop in the inner detector volume (stopping events) or continue through the inner detector (through-going events). All three data topologies are considered for this search. Further information about the event topologies, as well as the selection cuts used to identify them, can be found in Ashie et al. (2005).

A search window of ± 500 s around the LIGO detection time of each gravitational-wave event is selected. This is consistent with the time window chosen by the authors of Adrián-Martínez et al. (2016). Using data from 2339.4 days of livetime in SK, the number of neutrino events we expect to see in a 1000 s time window is $(9.41 \pm 0.07) \times 10^{-2}$ for the FC data set, $(7.52 \pm 0.23) \times 10^{-3}$ for the PC data set, and $(1.65 \pm 0.03) \times 10^{-2}$ for the UPMU data set. In the search window around both GW150914 and GW151226, no neutrino events were found in the FC, PC, or UPMU data sets. This null result is used in the calculation of the upper limit on neutrino fluence in the subsequent sections of this Letter.

2.2. Low-energy Data Sample

There are two neutrino event selection algorithms for the low-energy data sample: the supernova relic neutrino (SRN) search (Bays et al. 2012) and the solar neutrino analysis (Abe et al. 2016). The largest cross section in this energy region is the inverse beta decay of electron antineutrinos ($\bar{\nu}_e + p \rightarrow e^+ + n$). Neutrino elastic scattering ($\nu + e^- \rightarrow \nu + e^-$) is sensitive to all neutrino flavors, but dominated by electron neutrinos. The observable signal in the detector originates from the charged particle, i.e., positron or electron in these interactions. There are other charged-current and neutral-current interactions with ^{16}O nuclei that are subdominant.
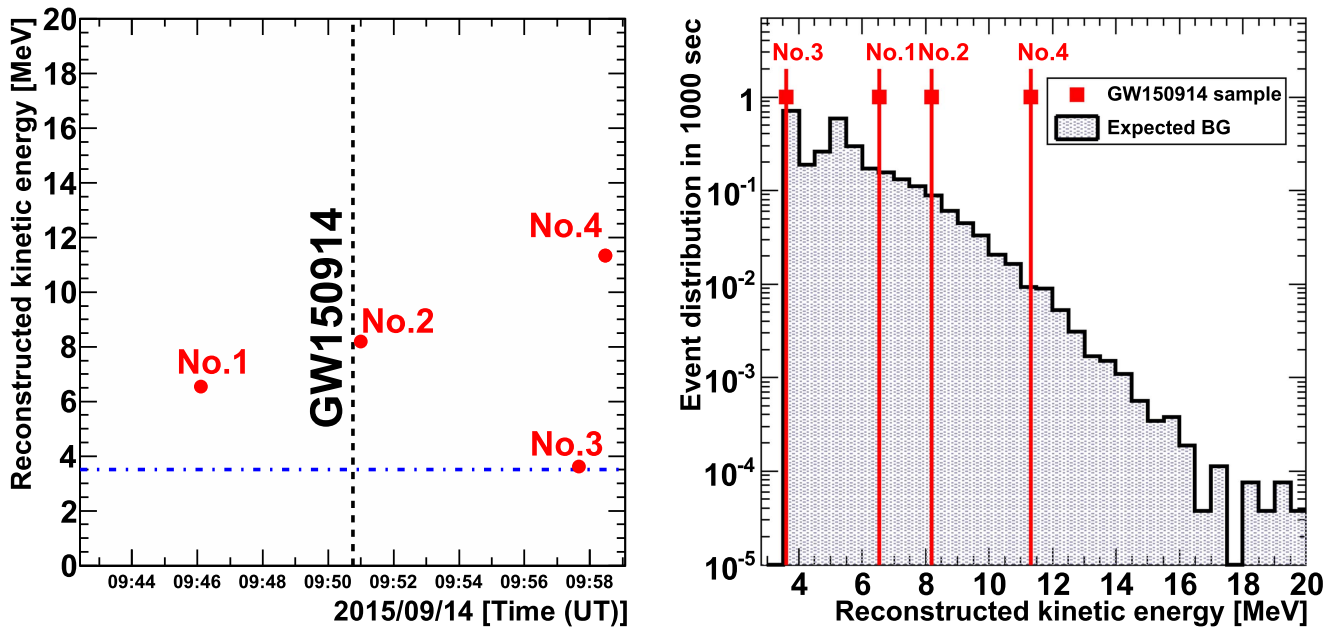
Figure 1. Detection time and the observed kinetic energy of the charged particle (left) and the energy spectrum with the expected background spectrum (right) after reduction cuts for the solar neutrino analysis are applied to the 1000 s search window around GW150914. The detection time of the four neutrino event candidates are as follows; No.1 9:46:07, No.2 9:51:00, No.3 9:57:40, No.4 9:58:28 UT. The energy threshold of this analysis, shown with the blue dashed line, is 3.5 MeV in kinetic energy.

The target energy range for the SRN analysis is from 15.5 to 79.5 MeV. Backgrounds relevant to the SRN analysis are atmospheric neutrino interactions (decay electrons from invisible muons, neutral-current interactions, low-energy pions and muons), solar neutrino interactions, and spallation products from cosmic-ray muons. The detailed analysis method and the reduction criteria are described in Bays et al. (2012), which, as well as this analysis, does not require a neutron capture in delayed coincidence (Zhang et al. 2015). After all the reduction steps, no neutino events are observed for the SRN analysis in the ±500 s search window around both GW150914 and GW151226. The expected number of background events in a 1000 s time window is $(1.45 \pm 0.09) \times 10^{-3}$ based on 1888.9 days of data. The absence of neutrino events in this energy region excludes the scenario of a coincidence between the gravitational-wave and a core-collapse supernova within a distance of 260 kpc at 90% C.L.

The energy region considered in the solar neutrino analysis is lower than that of the SRN search, from 3.5 to 19.5 MeV. The fluence calculation will be applied below 15.5 MeV to avoid double counting with the SRN sample. After applying all the reduction steps for the solar neutrino analysis, four neutrino event candidates remain within the ±500 s search window around the LIGO detection time of GW150914, while no neutrino event candidates remain around GW151226. Figure 1 shows the detection time and the energy of neutrino event candidates passing the reduction cuts for GW150914 (left) and the energy spectrum of the remaining events, which is consistent with the background spectrum (right). On 2015 May 1, the trigger threshold was changed from 34 observed PMT signals within 200 ns to 31 hits (Yamada et al. 2009; Nakano 2016). Using the data after that (306.6 days of livetime) we expect (2.90 ± 0.01) events due to random coincidence for each 1000 s time window centered around a gravitational-wave incident. For GW150914 the probability of seeing four or more events passing the reduction cuts is calculated to be 33.0%, the probability of seeing none for GW151226 is 5.5%. Therefore, our findings are consistent with all of these neutrino event candidates being background.

The background events in the solar neutrino analysis consist mainly of radioactive impurities below 5.5 MeV and spallation products above 5.5 MeV. The first and second events are most likely remaining spallation events caused by ^{16}N (Zhang et al. 2016). The transverse distance between each event and its preceding muon are 1.7 and 1.2 m, the timing differences between the event and the preceding muon are 10.77 and 17.38 s, and the energies are above 6 MeV, making these consistent with spallation production. Additionally, the likelihood value of the spallation product falls close to the cut value applied in the reduction steps. The expected number of background events above 5.5 MeV that survive the reduction cuts is (1.169 ± 0.007); therefore the probability of two or more events remaining in our sample is 32.6%. The third event is most likely a radioactive background event caused by the beta decay of ^{214}Bi from the radon decay chain. This is the dominant background near this energy region (3.6 MeV; Nakano 2016). The expected number of background events below 5.5 MeV that survive the reduction cuts is (1.735 ± 0.008); therefore, the probability that one or more events remains in our sample is 82.4%. The fourth event is most likely a solar neutrino event because the reconstructed direction is close to the solar direction (cosine of the angle between them $(\cos \theta_{Sun})$ is 0.96 with an angular resolution of 22.9°) and its recoil electron kinetic energy is 11.3 MeV, which is typical for solar neutrino event. The main background of this energy region is spallation events; however, the chance of accidental coincidence of these background events with the solar direction is quite small since the reduction of spallation events are already fairly efficient. The expected number of solar neutrino events is (0.229 ± 0.005) from the latest solar neutrino measurement in SK. The probability of one or more solar events remaining in our sample is 20.5%.
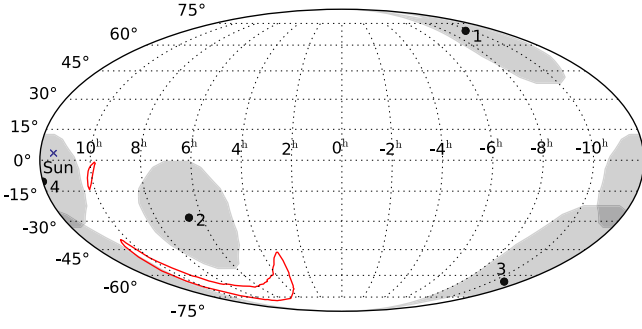
Figure 2. Reconstructed directions of the charged particle in the remaining four events associated with GW150914 (black points), shown here with the 90% CL contour for the location of GW150914 according to LALInterference data. The shaded area around SK events shows the 1σ angular resolution of the charged particle corresponding to the energy of each event. The "×" shows the Sun's direction at the time of the GW event.

Figure 2 shows the sky map using the reconstructed direction of the charged particle in the remaining four events associated with GW150914, along with the 90% CL contour for the location of GW150914 according to LALInterference data (Abbott et al. 2016b). The angular resolution of the charged particle is calibrated by electron LINAC (Nakahata et al. 1999). Because the energy spectrum and species of the incoming neutrinos is not known, an estimate of the angular uncertainty on the direction of the incoming neutrino is difficult; however, the direction of the charged particle has a strong correlation with the incident neutrino direction for the case of neutrino–electron scattering, while a very weak anti-correlation exists in the case of inverse beta decay (Strumia & Vissani 2003).

2.3. LVT151012

In addition to two gravitational-wave signals, LIGO reported a third binary black hole candidate with a smaller significance, named LVT151012, on 2015 October 12 at 09:54:43 UT (Abbott et al. 2016a). We also searched for a coincident neutrino signal within a ±500 s search window around the LVT151012 event. No neutrino events are found in the FC, PC, UPMU, and relic supernova neutrino data sample, while five neutrino event candidates remain after applying reduction steps for the solar neutrino analysis. The probability of five or more events remaining in the solar neutrino data sample is calculated to be 16.8%, which is also consistent with background events.

3. NEUTRINO FLUENCE LIMIT

The number of neutrino candidate events observed in the search window can be converted to an upper limit on neutrino fluence for both of the gravitational-wave events. This is done separately for the low-energy, FC+PC, and UPMU data sets. The procedure used to extract the fluence limit will be described briefly here, but uses the same prescription laid out in Thrane et al. (2009), which follows from Swanson et al. (2006).

For the FC and PC data set, the neutrino fluence can be calculated using Equation (1):

$$\Phi_{\mathrm{FC,PC}} = \frac{N_{90}}{N_T \int dE_\nu \, \sigma(E_\nu) \, \epsilon(E_\nu) \, \lambda(E_\nu^{-2})}, \quad (1)$$

where N_{90} is the 90% C.L. limit on the number of neutrino events in the search window calculated using a Poisson

distribution with a background, N_T is the number of target nuclei, σ is the combined cross section for all interactions particular to that neutrino flavor, ϵ is the efficiency for measuring the neutrino event in the detector, and λ is the number density of the events for a given energy spectrum with an index of -2. This spectral index is commonly used for astrophysical neutrinos accelerated by shocks (Gaisser et al. 1995). Since no neutrino candidate events pass cuts within the search window for the FC and PC data sets, we derive N_{90} using $N_{90} = -\ln(0.1) = 2.3$. Fluence limits are calculated separately for each neutrino species by considering the cross section and detection efficiency specific to the neutrino type.

Cross sections from NEUT 5.3.5 (Hayato 2009) are used in the calculation of Equation (1). To determine the detector efficiency, mono-energetic neutrino interaction files produced with NEUT 5.3.5 are passed as inputs to the SK Monte Carlo detector simulation. The resulting output files then undergo the same reconstruction and reduction procedures that are applied to the data. The efficiency is determined by calculating the fraction of remaining events after reduction and selection cuts. The energy range of 100 MeV–10 GeV is considered.

For the UPMU data set, the neutrino fluence is calculated using Equation (2):

$$\Phi_{\mathrm{UPMU}} = \frac{N_{90}}{A_{\mathrm{eff}}(z) \int dE_\nu \, P(E_\nu) \, S(z, E_\nu) \, \lambda(E_\nu^{-2})}. \quad (2)$$

Here, fluence depends on the zenith-dependent effective area ($A_{\mathrm{eff}}(z)$), where z is the zenith angle of the incoming neutrino, the probability for a neutrino to create a muon with energy greater than $E_\nu^{\min}$ ($P(E_\nu)$), the shadowing of the neutrinos due to interactions in the Earth ($S(z, E_\nu)$), and the number density (λ) of the neutrino events for the given energy spectrum with an index of -2. Again, since there are no neutrino candidate events within the search window for the UPMU data set, we use $N_{90} = 2.3$. The energy range considered for the UPMU fluence is 1.6 GeV–100 PeV.

For the low-energy data sample, the neutrino fluence calculation is similar to Equation (1); however, since there is no reason to assume a power spectrum nor any reliable theory of neutrino emission spectrum in this energy region, we set the neutrino energy spectrum to have an index of 0, which is flat. Therefore, the fluence limit is calculated with the assumption of flat spectrum of neutrino energy from 3.5 to 75 MeV as shown in Equation (3):

$$\Phi_{\mathrm{lowe}} = \frac{N_{90}}{N_T \int dE_\nu \, \lambda(E_\nu) \, \sigma(E_\nu) \, R(E_e, E_{\mathrm{vis}}) \, \epsilon(E_{\mathrm{vis}})}, \quad (3)$$

where R is the response function from electron or positron energy (E_e) to the kinetic energy in SK (E_{vis}). The response function and the detection efficiency (ϵ) is calculated using the SK detector Monte Carlo simulation. N_{90} is calculated to be 5.41 (2.30) from the remaining four (zero) neutrino candidate events compared to the expected 2.90 events in this data sample for GW150914 (GW151226). The accidental coincidence of solar neutrinos with a gravitational-wave signal are easily reduced by a factor of 0.9 with an angular cut on the recoil electron's direction ($\cos\theta_{\mathrm{Sun}} > 0.8$). In this case, the number of remaining neutrino candidate events is three (zero) compared to 2.46 expected events, and N_{90} is 4.64 (2.30) for GW150914
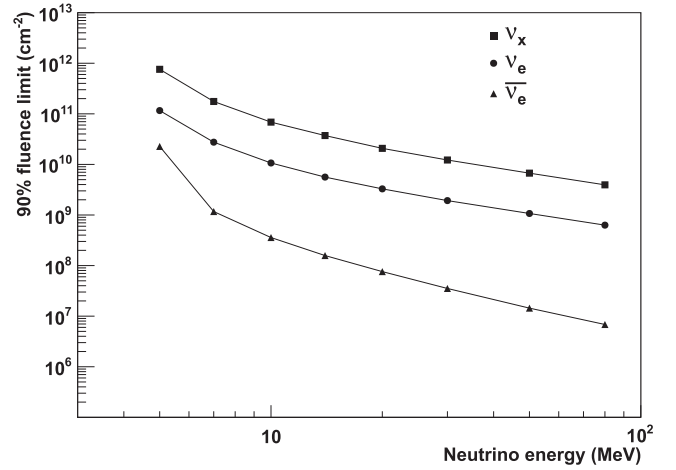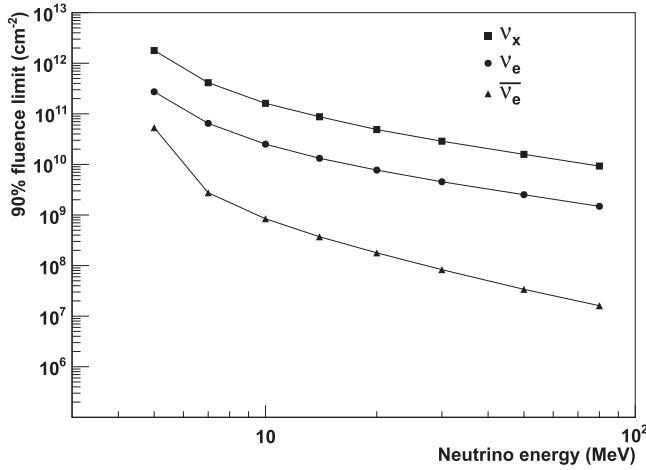
Figure 3. The 90% C.L. limit for GW150914 (left) and GW151226 (right) on fluence obtained by mono-energetic neutrinos at different specific energies from the low-energy data sample.

(GW151226). In addition, since any emission models for low-energy neutrinos are not well motivated, we express the fluence limit that is calculated for monochromatic neutrino energy E_ν obtained by replacing $\lambda(E_\nu)$ with a delta function $\delta(E - E_\nu)$. The fluence limits for both GW events are shown in Figure 3.

Table 1 shows the fluence limit results for the FC+PC, UPMU, and low-energy data sets for both gravitational-wave events separately, as well as for both events combined. To calculate the combined neutrino fluence limit, the N_{90} is calculated using the search windows around both gravitational-wave events and is then weighted by the number of gravitational-wave events, which in this case is two. For the UPMU events, fluence is dependent on zenith angle, and thus we show the upper limit of neutrino fluence from UPMU events as a sky map of possible fluence limits in Figure 4. Since the gravitational-wave events are not well localized, a combined fluence limit for the UPMU data set is not reported. The UPMU upper limit fluence values range from $(14-37)\,\mathrm{cm}^{-2}$ for neutrinos and from $(19-50)\,\mathrm{cm}^{-2}$ for antineutrinos, depending on the direction of the gravitational-wave event. We convert our UPMU fluence limit to an upper limit on total energy radiated in neutrinos by convolving Equation (2) by the energy spectrum and weighting by $4\pi d_{\mathrm{GW}}^2$ where d_{GW} is the distance between the detector and the gravitational-wave source. The resulting upper limit on total energy is $E_\nu^{\mathrm{tot}} \sim (1-6) \times 10^{55}\,\mathrm{erg}$ for GW150914 assuming the LIGO-determined distance of 410 Mpc and $E_\nu^{\mathrm{tot}} \sim (2-7) \times 10^{55}\,\mathrm{erg}$ for GW151226 assuming the LIGO-determined distance of 440 Mpc. For comparison, the total energy radiated in gravitational waves by GW150914 is $\sim 5 \times 10^{54}\,\mathrm{erg}$ (Adrián-Martínez et al. 2016), and the total energy radiated in neutrinos from a typical supernova is $\sim$ a few $\times 10^{53}\,\mathrm{erg}$ (Bethe 1990).

4. CONCLUSION

We search for possible neutrino signals coincident with GW150914, GW151226, and LVT151012 in the SK detector using a wide energy range from 3.5 MeV to 100 PeV. In the high-energy data sample, three neutrino interaction categories are considered: FC, PC, and UPMU. No neutrino candidate events are found in the search window of $\pm 500\,\mathrm{s}$ around the LIGO detection time for both gravitational-wave signals.

Table 1
Limits at 90% C.L. on the Fluence of Neutrinos from GW150914 and GW151226 Given a Spectral Index of -2 and an Energy Range of 100 MeV–10 GeV for the FC+PC and 1.6 GeV–100 PeV for the UPMU Data Samples, and a Flat Spectrum for the Low-energy Data Sample whose Energy Region Is from 3.5 to 75 MeV

	GW150914 Φ_ν (cm^{-2})	GW151226 Φ_ν(cm^{-2})	Combined Φ_ν (cm^{-2})
	From FC+PC only		
ν_μ	5.6×10^4	5.6×10^4	2.8×10^4
$\bar{\nu}_\mu$	1.3×10^5	1.3×10^5	6.5×10^4
ν_e	4.8×10^4	4.8×10^4	2.4×10^4
$\bar{\nu}_e$	1.2×10^5	1.2×10^5	6.0×10^4
	From UPMU only		
ν_μ	14–37	14–37	…
$\bar{\nu}_\mu$	19–50	19–50	…
	From low-energy only		
$\bar{\nu}_e$	$4.2/3.6 \times 10^7$	$1.8/1.8 \times 10^7$	$1.6/1.5 \times 10^7$
ν_e	$3.0/2.6 \times 10^9$	$1.3/1.3 \times 10^9$	$1.2/1.1 \times 10^9$
ν_x	$1.9/1.6 \times 10^{10}$	$8.1/8.1 \times 10^9$	$7.0/7.0 \times 10^9$

Note. The values on the left/right in the low-energy sample show the fluence limit without/with the solar direction cut, respectively.

Low-energy neutrino events are also examined using the SRN and the solar neutrino data samples in the same search time window. No neutrino candidate events are found in the SRN data sample for both gravitational-wave signals. No neutrino candidate events are found in the solar neutrino data for GW151226; however, four neutrino candidate events are found for GW150914. These four events are consistent with the estimated background, with one of them possibly associated with solar neutrinos.

The obtained neutrino fluence limits give the most stringent limits for neutrino emission in the energy region below $\sim 100\,\mathrm{GeV}$, assuming an E^{-2} spectrum from GW150914 and GW151226. The absence of MeV neutrino emission in the solar neutrino and the SRN data samples is inconsistent with the source of the gravitational-wave signals being a nearby core-collapsed astronomical object.
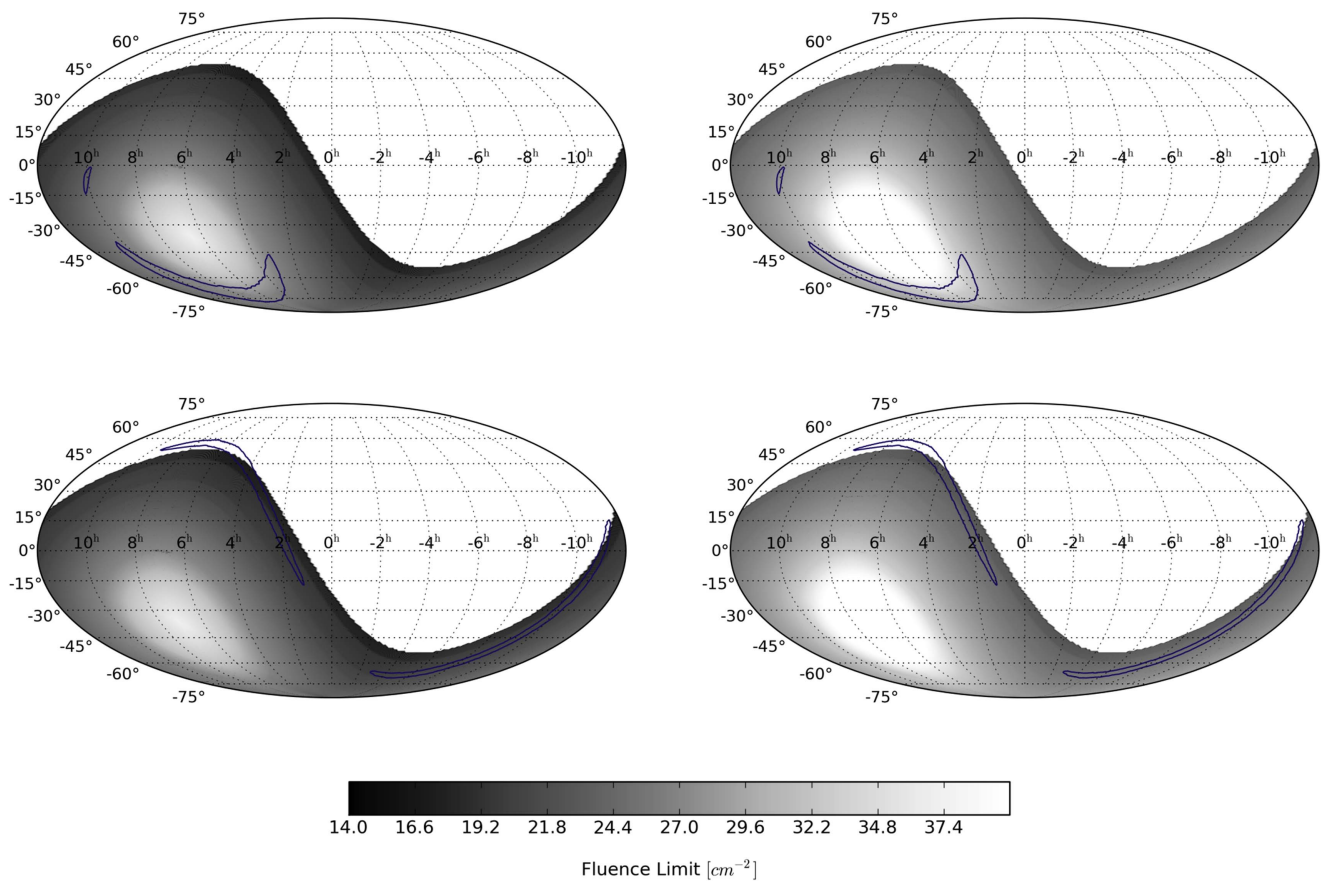
Figure 4. The 90% C.L. limit on fluence for neutrinos considering only the UPMU data set, overlaid with the 90% C.L. contour for the location of the gravitational-wave event according to LALInterference data (solid blue line). The upper (lower) panel shows the information for GW150914 (GW151226), and the left (right) panel shows the information for neutrinos (antineutrinos). For this limit, an energy range of 1.6 GeV–100 PeV was used.

REFERENCES

Abbott, B. P., Abbott, R., Abbott, T. D., et al. 2016a, PhRvL, 116, 241103
Abbott, B. P., Abbott, R., Abbott, T. D., et al. 2016b, ApJL, 826, L13
Abbott, B. P., Abbott, R., Abbott, T. D., et al. 2016c, PhRvL, 116, 061102
Abe, K., Haga, Y., Hayato, Y., et al. 2016, PhRvD, 94, 052010
Adrián-Martínez, S., Albert, A., André, M., et al. 2016, PhRvD, 93, 122010
Ashie, Y., Hosaka, J., Ishihara, K., et al. 2005, PhRvD, 71, 112005
Bays, K., Iida, T., Abe, K., et al. 2012, PhRvD, 85, 052007
Bethe, H. A. 1990, RvMP, 62, 801
Connaughton, V., Burns, E., Goldstein, A., et al. 2016, ApJL, 826, L6
Eichler, D., Livio, M., Piran, T., & Schramm, D. N. 1989, Natur, 340, 126
Fukuda, S., Fukuda, Y., Hayakawa, T., et al. 2003, NIMPA, 501, 418
Gaisser, T. K., Halzen, F., & Stanev, T. 1995, PhR, 258, 173 [Erratum: 1996, PhR, 271, 355]
Gando, A., Gando, Y., Hachiya, T., et al. 2016, arXiv:1606.07155
Greiner, J., Burgess, J. M., Savchenko, V., & Yu, H.-F. 2016, arXiv:1606.00314
Hayato, Y. 2009, AcPP, B40, 2477
Nakahata, M., Fukuda, Y., Hayakawa, T., et al. 1999, NIMPA, 421, 113
Nakano, Y. 2016, PhD thesis, Univ. Tokyo
Strumia, A., & Vissani, F. 2003, PhLB, 564, 42
Swanson, M. E. C., Abe, K., Hosaka, J., et al. 2006, ApJ, 652, 206
Thrane, E., Abe, K., Hayato, Y., et al. 2009, ApJ, 704, 503
Woosley, S. E. 1993, ApJ, 405, 273
Yamada, S., Awai, K., Hayato, Y., et al. 2009, ITNS, 57, 428
Zhang, H., Abe, K., Hayato, Y., et al. 2015, APh, 60, 41
Zhang, Y., Abe, K., Haga, Y., et al. 2016, PhRvD, 93, 012004